

De-risking solutions to optimization problems*

Daniel Bienstock and Blake Sisson, Columbia University

May 28, 2026

Abstract

We develop a cutting-plane methodology that adjusts solutions to optimization problems so as to reduce features that bring about exposure to risk, such as concentration of assets or resources. The methodology is agnostic to the representation of risk. Our procedure aims to reduce the appropriate risk metric without accruing a significant increase in nominal cost, rapidly, or proves that such an adjustment is not possible. The underlying approach borrows from techniques used in first-order methods for optimization.

1 Introduction

Consider a generic optimization problem

$$\min c(x), \text{ s.t. } x \in P. \quad (1)$$

An empirical fact which is found in many real-world settings is that optimal or near-optimal solutions end up, inadvertently, exposed to *risk*, the precise nature of which may be quite poorly understood. Our perspective is motivated using examples of optimization in a number of logistical and planning settings we encounter through applications.

In particular, we find that an optimal solution to the nominal problem (1) may incorporate high *concentration* or *congestion*, for example, by placing a large percentage of high-value items in a small set of locations during a narrow time span, causing exposure to many different types of actual risk that are difficult to precisely and comprehensibly quantify.

Notably, a concrete numerical representation for risk may both be high-dimensional and rely on units and attributes not explicitly present in (1); see the examples below. As a simple example, a high volume of commodities routed on network arcs across a cut at a given point in time is aligned with increased likelihood for congestion – the causes and actual impact of may be difficult to quantify. In fact, congestion can be compounded by features external to problem (1) which exhibit adversarial or stochastic behavior, for example by reducing the capacities of certain arcs when congestion on those arcs is high.

In this paper we will assume that risk is approximately quantified through a function $\Phi(x)$. To fix ideas we will refer to $\Phi(x)$ as the *impact* function, which should be seen as a representation of exposure to or outcome from uncertainty that is outside the scope of problem (1) but can significantly degrade the attractiveness of solutions. We stress that $\Phi(x)$ only amounts to an approximate representation of risk, and that its numerical representation may be high-dimensional.

The algorithms discussed in this paper efficiently probe the frontier defined by cost versus impact, in order to rapidly de-risk an optimal solution x^* to (1) by either

*Funded by AFOSR and ONR.

- (a) computing an alternative vector $\hat{x} \in P$ with *significantly lower risk but moderate increase in cost* relative to x^* , or
- (b) proving that no such vector exists.

Thus, in simple terms, we develop computational tools that support an *optimistic* risk-tolerance stance, when possible, and that yield at least a partial explanation (i.e., an impossibility proof) when not achievable.

1.1 Motivation

The plot in Figure 1 was produced by solving a logistical MIP that models shipping a variety of commodities using several vehicle types on a medium-sized network in a multiperiod setting. The model is endowed with several types of capacities, vehicle availabilities, deadlines and vehicle-commodity compatibility rules. The particular case considered here has over 400,000 variables of which over 5,000 are integral.

Figure 1 displays sorted *activity* weights – an activity is the set of all shipments on a given network link at a given point in time, over all available vehicles. Even though there are over 10,000 such activities, only approximately 150 are nonzero at the optimum. More significantly, we see very high concentration near the top.

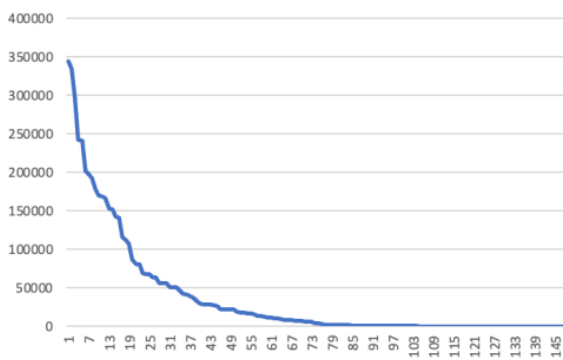


Figure 1: Sorted activity weights.

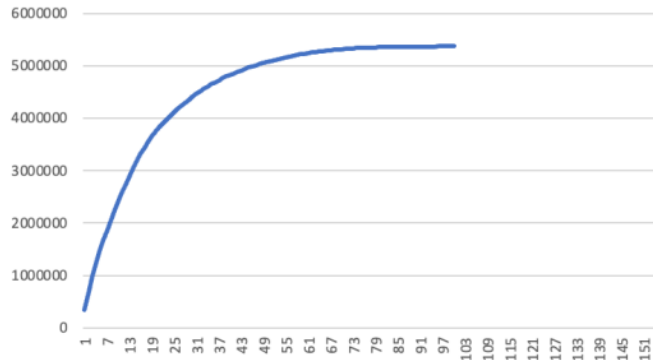


Figure 2: Aggregate worth of top activities.

To obtain Figure 2 we considered, for each activity, i.e., each network link and time period, the total *worth* of commodities shipped on that link in that time period using all available vehicles – each commodity type has a certain worth, or value. The figure plots the aggregate worth of the top K activities, for $K = 1, 2, \dots$

Note, again, the high concentration. For example, the top ten worth activities account for approximately 40% of all shipped worth. Such concentration is risk-inducing in an intuitive fashion: congestion or an adversarial event that affects a small number of high-worth activities will be of negative impact out of proportion to the number of such activities.

1.1.1 Discussion of potential approach

A mathematically correct approach for our de-risking goal is to address formulations of the form

$$\min c(x) \tag{2a}$$

$$\text{s.t. } x \in P, \tag{2b}$$

$$\Phi(x) \leq \Lambda, \tag{2c}$$

where Λ is an input parameter that overtly expresses a decision-maker’s tolerance for risk. We do not favor this methodology for three reasons detailed next.

1. Problematic selection for Λ . A priori, it may not be clear what value Λ should take because. A major issue is that any choice for Λ reflects a risk-tolerance stance, and, ideally, one should estimate an efficient frontier by enumerating multiple values Λ . The salient point is that the solution (vector and value) to (2) may be very sensitive to the choice of Λ especially in nonlinear, nonconvex cases. At any rate, it is the corrective goal mentioned above; de-risking an optimal solution to (1), that is of interest to us, and not a specific choice of an impact upper-bound Λ . Our de-risking goal is explicitly imprecise but allows for an *approximate* and implicit choice for Λ that is supported by a rigorous argument. See Lemma 2.9.

2. Computational challenges arising from an explicit choice for Λ . An additional hazard arises from a computational standpoint: a choice that is aggressive – Λ is too small– would cause problem (2) to become infeasible or nearly so. In fact the computation of the smallest value Λ such that (2) remains feasible can be a nontrivial problem even in cases where (1) is a linear program¹. If (2) is at the boundary of feasibility, solution time could be unacceptably lengthy or the solver tackling (2) might simply fail, while, potentially, a slightly larger choice yields a much faster solution.

3. An overly complex and large formulation. The explicit representation of $\Phi(x)$ in (2c) might require a formulation of great complexity and unacceptably large size, causing problem (2) to become far more challenging than (1). The problem in Figures 1 and 2 is an example of this behavior. More broadly, this could already be the case in a non-adversarial setting when $\Phi(x)$ is nonlinear and expresses many features at risk but especially so in the adversarial case. In selected cases (e.g., when a convex relaxation is available) a cutting-plane approach might be tenable, however, it would be exposed to the issues detailed in the above paragraphs, e.g., a poor choice for Λ .

1.1.2 Our approach

We present a family of procedures that approximately solve impact-weighted formulations

$$\min c(x) + \Theta \Phi(x) \tag{3a}$$

$$\text{s.t. } x \in P, \tag{3b}$$

where $\Theta > 0$ is a risk-aversion parameter. Our approximation goal is driven by the following:

- (a) The procedures aim to de-risk an optimal solution x^* to the nominal problem (1), i.e., to compute $\hat{x} \in P$ with small increase in cost together with large decrease in impact, both relative to x^* . While this goal obviously cannot always be attained (e.g., because of structure of P), our empirical experience indicates that it is frequently achievable in relevant cases.

¹It includes the min-cut problem as a special case.

- (b) The procedure was chosen to facilitate (a) and will only yield approximately optimal but feasible solutions to (3). The theoretical guarantees we provide address this approximation.

The value Θ must, of course, be selected: we will provide method to address this issue that is provably correct with regards to goal (a) above. And, to some extent, a choice for Θ implies an equivalent choice for Λ in (2) – however, this equivalence only applies to formally optimal solutions to the respective problems and formulation (3) proves more flexible than (2) when an approximate answer is desired.

In the above descriptions, the impact function $\Phi(x)$ is presented in abstract form which potentially includes an adversarial ingredient. It will be beneficial to further specify such a setting, as follows. We are given a compact set \mathcal{Z} that parameterizes uncertainty, and for each $z \in \mathcal{Z}$, we have a realization of the impact function of the form $\Phi(x|z)$. This notation captures purely stochastic forms of risk such as moments or tail probabilities as well as robust (worst-case) risk representations. The adversarial setting can therefore be summarized by writing

$$\Phi(x) = \max_{z \in \mathcal{Z}} \Phi(x|z). \quad (4)$$

We assume that for each $x \in P$ and $z \in \mathcal{Z}$, $\Phi(x|z) \geq 0$.

As an example of this modeling device in the logistical setting given above, consider a family of joint distributions \mathcal{Z} , each of which describes an uncertain event that results in capacity loss in network links. The risk-aligned quantity of interest, here, would be a measure of the amount of worth of flow that is delayed or lost under distribution $z \in \mathcal{Z}$. We will expand on this example below.

1.2 Review of prior work

The perspective we take in this paper concerns risk arising from solutions to optimization problems that incorporate concentration, in a generic sense. One of the earliest citations in this context is [18], which concerned routing problems (in packet networks) that can formally be stated as linear optimization problems. However, congestion brings about the risk of queueing delays: let the flow on an arc with capacity u be x : then the M/M/1 queueing delay is $u/(u-x)$ (see, e.g., [24]). The combinatorial algorithm in [18] approximately solves an optimization problem whose objective function is the original cost function, plus the sum of all queueing delays, thus trading-off cost versus queueing risk (i.e., delays).

A related problem was later taken up in [29]. They consider a capacity-constrained multi-commodity flow routing problem, where the capacities are insufficient to route all commodities. Under such conditions, the algorithm in [29] computes a routing that approximately minimizes the maximum overload in any arc, which is defined as the ratio of flow to capacity. The algorithm replaces this min-max task, with an approximately equivalent nonlinear optimization problem which is (again, approximately) handled using a first-order method.

This approach was greatly extended and improved in [27], and [19]. Let \mathcal{A} denote the set of arcs in a multicommodity flow network, and for an arc $(i, j) \in \mathcal{A}$, let u_{ij} denote its capacity, and for a (multicommodity) flow vector f let f_{ij} denote the sum of commodity flows routed on (i, j) . Then the min-max routing problem described in the above paragraph can be stated as

$$\min_{f \in \mathcal{F}} \max_{(i,j) \in \mathcal{A}} f_{ij}/u_{ij}, \quad (5)$$

where \mathcal{F} is the set of feasible flows, i.e., all flows that deliver all commodities from their source to their destination, possibly exceeding capacities. On very large networks with many commodities

this optimization problem, which can be stated as a linear program, proves quite challenging to modern LP solvers. In contrast, [27] and [19] show that the min-max problem can approximately be modeled using an appropriate nonlinear *potential function* as a proxy:

$$\min_{f \in \mathcal{F}} \ln \left(\sum_{(i,j) \in A} e^{\alpha f_{ij}/u_{ij}} \right). \quad (6)$$

More precisely, given $0 < \varepsilon < 1$, choosing α appropriately (primarily, α proportional to ε^{-1}) a solution to the potential function problem (6) yields a flow vector f that is ε -optimal to the min-max problem (5). Moreover, the approximate minimization in (6) is carried out, effectively, via a first-order method where individual iterations amount to linear programs whose objective is the gradient of the function in (6). We will rely on a similar proxy in our work, though our algorithmic goals and methodology are quite different.

As a function of ε , the number of iterations needed to obtain an ε -optimal solution to (5) grows proportional to $1/\varepsilon^2$ (later improved to $1/\varepsilon$, [10]). See [9] for an analysis of [18], [27] and [19] and follow-up work that improved on these algorithms, as well as computational experiments.

Our risk perspective can include an exogenous adversarial component. There is a very large literature of models for *interdiction* that take an adversarial standpoint: how to optimally or maximally disrupt, e.g., a logistical operation. In this regard, the case of a network under stochastic capacity interdiction is studied in [17] (also see references therein). This work considers a variety of models where an adversary interdicts arcs of a network by reducing their capacity under various assumptions of likelihood of success of interdiction and of capacity reduction, as well as adversarial capabilities; and produces efficient formulations for such problems. Optimization problems where under the risk of adversarial interdiction are often handled using a cutting-plane algorithm that is reminiscent of (or equivalent to) Benders' decomposition [4]. Related problems are considered in [12].

A salient and challenging application of interdiction analysis involves the so-called $N - K$ problem in power grids; see [28], [11]. Briefly, an operational constraint in modern power grids is that *any* simultaneous disablement of up to K components (e.g., arcs) should be tolerated by the system; here $K > 0$ is a small integer. The case $K = 1$ is enshrined as law in many countries, but larger values of K are becoming relevant. Note that the enumeration of all subsets of size K is infeasible even for relatively small K (e.g., 3) when the grid is large, and a generic Benders' approach, when applicable, proves invaluable.

Optimization problems under interdiction risk are usually (if unwittingly) modeled as bilevel optimization problems, for which there is also a very abundant literature. Bilevel optimization problems are complex and Benders' decomposition is not always an easy or even feasible task (and its misapplication can lead to wrong algorithms). For a recent survey, see [3].

Finally, the incorporation of an adversarial model can bring about the robust optimization perspective, especially in the so-called "risk-budgets" setup. See [6] and [5]. Many of the previously cited works on interdiction models can be seen through the lens of risk budgets.

2 Algorithms

In this section we describe several cutting-plane algorithms for problem (3) in its adversarial form (4) that rely on its epigraph representation

$$\min c(x) + \Theta \phi_L \quad (7a)$$

$$\text{s.t. } x \in P, \quad (7b)$$

$$\phi_L \geq \max_{z \in \mathcal{Z}} \Phi(x|z), \quad (7c)$$

where ϕ_L is an auxiliary variable.

2.1 Formal setup with risk features

The problem setup we will consider have the following characteristics. As inputs, we have

- (a) A set I of nonnegative-valued functions of the form $\phi_i(x|z)$ ($i \in I$). We assume that I is finite though potentially very large. We will refer to the ϕ_i as the *features*. Each feature is a function of the decision vector x as well as the exogenous risk-inducing vector $z \in \mathcal{Z}$.
- (b) A set of values $\lambda_1 \geq \dots \geq \lambda_{|I|} \geq 0$ with $\sum_{i=1}^{|I|} \lambda_i = 1$. We focus on the following version of (7):

$$\min c(x) + \Theta \phi_L \quad (8a)$$

$$\text{s.t. } x \in P, \quad \phi_L \geq \max_{z \in \mathcal{Z}} \sum_{k=1}^{|I|} \lambda_k \phi_{(k)}(x|z). \quad (8b)$$

Here $\phi_{(k)}(x|z)$ is the k^{th} largest value $\phi_i(x|z)$.

Denote by $\mathcal{S}_{|I|}$ the set of permutations of $|I|$ entities, and for $\pi \in \mathcal{S}_{|I|}$ (with a slight abuse of notation) use $\pi(i)$ to denote the corresponding element i of I . Thus, for $x \in P$ and $z \in \mathcal{Z}$, we have

$$\sum_{k=1}^{|I|} \lambda_k \phi_{(k)}(x|z) = \max_{\pi \in \mathcal{S}_{|I|}} \sum_{k=1}^{|I|} \lambda_k \phi_{\pi(k)}(x|z). \quad (9)$$

In particular, when $\lambda_k = 0$ for $k > 1$ problem (8) becomes

$$\min c(x) + \Theta \phi_L \quad (10a)$$

$$\text{s.t. } x \in P, \quad \phi_L \geq \max_{z \in \mathcal{Z}} \max_{i \in I} \phi_i(x|z). \quad (10b)$$

Using (9), we note that (8) is, in fact, a *special case* of (10) with appropriately defined and exponentially many new features (e.g., one for each $\pi \in \mathcal{S}_I$). For *simplicity of language*, in the theoretical results below we assume the form (10).

2.2 Prototype algorithm

Here we describe a procedure, Algorithm 1, which has provable convergence attributes. It serves as a common intellectual core for a family of procedures that prove empirically successful. These procedures, which are discussed in Section 2.4.3, incorporate pragmatic modifications to Algorithm 1 for high-dimensional cases and in some cases are also endowed with provably correct attributes.

Algorithm 1 SOFTMAX-ADVERSARIAL

- 1: **Inputs:** $t^{\max} > 0$ (max. no. of iterations), $\Theta > 0$; $\alpha > 0$; Δ, δ, Δ' (positive tolerances).
- 2: Set $t = 0$, and initialize the *master problem* as

$$\min c(x) + \Theta \phi_L, \quad \text{s.t. } x \in P, \phi_L \geq 0.$$

- 3: **while** $t < t^{\max}$ **do**:
- 4: Solve the master problem; let (x^t, ϕ_L^t) be an optimal solution.
- 5: **Boosting step.** Compute $z^t \in \mathcal{Z}$ such that

$$\ln \sum_{i \in I} e^{\alpha \phi_i(x^t | z^t)} \geq \max_{z \in \mathcal{Z}} \ln \sum_{i \in I} e^{\alpha \phi_i(x^t | z)} - \Delta'.$$

Define $\phi_{\max}^t = \max_{i \in I} \phi_i(x^t | z^t)$.

- 6: **if** (a) $\phi_{\max}^t \leq \phi_L^t + \Delta$, or (b) $\phi_{\max}^t - \phi_L^t \leq \delta \phi_{\max}^t$ **then STOP**.
 - 7: **else**
 - 8: For each $i \in I$ write $\pi_i^t = \frac{e^{\alpha \phi_i(x^t | z^t)}}{\sum_{j \in I} e^{\alpha \phi_j(x^t | z^t)}}$
 - 9: **Separation.** Add the cut $\phi_L \geq \sum_{i \in I} \pi_i^t \phi_i(x | z^t)$ to the master problem.
 - 10: **end if**
 - 11: $t \leftarrow t + 1$.
 - 12: **end while**
-

2.3 Preliminary discussion of Algorithm 1

For $x \in X$ write

$$\phi_U(x) = \max_{z \in \mathcal{Z}} \max_{i \in I} \phi_i(x | z),$$

i.e., the right-hand side of constraint (10b). Consider any iteration $t \geq 0$. Note that $\pi^t \geq 0$ and $\sum_i \pi_i^t = 1$. As we will see below (Lemma 2.1), this implies $\phi_L^t \leq \phi_U(x^t)$, and, as a result, the master problem is always a relaxation of (10). Moreover,

- $\phi_U^t - \phi_L^t$ amounts to the infeasibility of (x^t, ϕ_L^t) in problem (10) – should this quantity be small, the algorithm will have converged to an approximate optimal solution.
- By definition $\phi_{\max}^t \doteq \max_{i \in I} \phi_i(x^t | z^t) \leq \phi_U(x^t)$,
- Furthermore (Lemma 2.2), $\phi_U(x^t) \leq \phi_{\max}^t + 2\Delta$.

In summary, ϕ_{\max}^t is a valid proxy to $\phi_U(x^t)$, and, as a result, the stopping conditions in line 6 are numerically valid termination conditions for the cutting plane algorithm (absolute and relative, resp.). In order for this statement to be mathematically valid we need that δ be small in absolute terms, e.g., $\delta = 10^{-6}$, and that Δ be small in relative terms, i.e. $\Delta \leq 10^{-6} \phi_{\max}^t$. In the numerical implementation of Algorithm (1) we will relax these conditions in order to allow early termination, in line with our 'de-risking' goal. Also see Theorem 2.8.

Remark. In machine learning language, the function optimized in line 5 of the algorithm is known as *log-sum-exp*, while the cut coefficients in line 8 follow the *softmax* function. Formally, given $y \in \mathbf{R}^n$, and $\alpha > 0$ we write

$$\text{SOFTMAX}(\alpha, y)_i \doteq \frac{e^{\alpha y_i}}{\sum_{j=1}^n e^{\alpha y_j}}.$$

It is seen that the softmax function is proportional to the gradient of log-sum-exp (in feature space), that is to say, defining $\phi = (\phi_i, i \in I)$, $L(\phi) = \ln \sum_{i \in I} e^{\alpha \phi_i}$ and $g(\phi)$ as the vector with entry $g_i(\phi) = \alpha \frac{e^{\alpha \phi_i}}{\sum_{j \in I} e^{\alpha \phi_j}}$ for each $i \in I$, we have $\nabla_{\phi} L(\phi) = g(\phi)$.

As defined, L is a convex function of ϕ . Thus, given a particular vector $\bar{\phi}$ it holds that

$$L(\phi) \geq g^T(\bar{\phi})(\phi - \bar{\phi}) + L(\bar{\phi}). \quad (11)$$

Using this observation, one can write a modification to Algorithm 1 similar to Kelley's [22] algorithm using the outer-approximation cuts (11) instead of the cuts added in line 9.

2.4 Analysis of Algorithm 1

We next present results regarding the convergence properties of Algorithm 1. In any iteration t , write $\phi_U^t \doteq \phi_U(x^t)$, i.e., $\max_{z \in \mathcal{Z}} \max_{i \in I} \phi_i(x^t|z)$ according to our notation above. We will set $\Delta' = \alpha \Delta$ with $\alpha \geq \frac{\ln|I| + \ln(2\phi_U^0/\Delta)^+}{\Delta}$, which is well-defined since α is not actually needed until the first execution of line 5, i.e., not until after x^0 is computed.

Lemma 2.1 *At any iteration t , $\phi_L^t \leq \phi_U^t$.*

PROOF: This is true for $t = 0$ since $\phi_L^0 = 0$, and for $t > 0$ we have that (since $\Theta > 0$), $\phi_L^t = \sum_{i \in I} \pi_i^{t'} \phi_i(x^t|z^{t'})$ for some $t' < t$. Since the $\pi_i^{t'}$ are nonnegative and sum to 1 the proof is complete. ■

Lemma 2.2 *At any iteration t , $\phi_U^t \leq \phi_{\max}^t + 2\Delta$.*

PROOF: Given $z \in \mathcal{Z}$, $e^{\alpha \max_{i \in I} \phi_i(x^t|z)} \leq \sum_{i \in I} e^{\alpha \phi_i(x^t|z)} \leq |I| e^{\alpha \max_{i \in I} \phi_i(x^t|z)}$ and therefore

$$\alpha \max_{i \in I} \phi_i(x^t|z) \leq \ln \sum_{i \in I} e^{\alpha \phi_i(x^t|z)} \leq \ln |I| + \alpha \max_{i \in I} \phi_i(x^t|z). \quad (12)$$

So

$$\alpha \phi_U^t \leq \max_{z \in \mathcal{Z}} \ln \sum_{i \in I} e^{\alpha \phi_i(x^t|z)} \leq \ln \sum_{i \in I} e^{\alpha \phi_i(x^t|z^t)} + \Delta',$$

as per line 5 of the algorithm. Using (12) with $z = z^t$, this quantity is at most $\ln |I| + \Delta' + \alpha \phi_{\max}^t$. In summary, $\phi_U^t \leq \frac{\ln |I| + \Delta'}{\alpha} + \phi_{\max}^t \leq \phi_{\max}^t + 2\Delta$ by definition of α and Δ' . ■

Corollary 2.3 *Suppose the algorithm terminates at iteration t (line 6). If criterion (a) applies, $\phi_U^t - 3\Delta \leq \phi_L^t \leq \phi_U^t$. And if (b) applies $(1 - \delta)\phi_U^t - 2\Delta \leq \phi_L^t \leq \phi_U^t$.*

PROOF: This follows from the termination condition, Lemmas 2.1 and 2.2. ■

Observation 2.4 *Given t , let $\tilde{x} \in P$ be such that $c(\tilde{x}) < c(x^t)$. Then $\max_{z \in \mathcal{Z}} \max_{i \in I} \phi_i(\tilde{x}|z) > \phi_L^t$.*

This follows because $(\tilde{x}, \max_{z \in \mathcal{Z}} \max_{i \in I} \phi_i(\tilde{x}|z))$ is feasible for the master problem at iteration t . In light of Corollary 2.3, this shows that even prior to termination, the algorithm yields useful information.

Lemma 2.5 *For any t , $\phi_L^t \leq \phi_U^0$.*

PROOF: For any $x \in P$, the pair $(x, \max_{z \in \mathcal{Z}} \max_{i \in I} \phi_i(x|z))$ is feasible for the master problem at iteration t . Using this fact with $x = x^0$, we get

$$c(x^t) + \Theta \phi_L^t \leq c(x^0) + \Theta \max_{z \in \mathcal{Z}} \max_{i \in I} \phi_i(x^0|z) = c(x^0) + \Theta \phi_U^0.$$

Since by construction $c(x^0) \leq c(x^t)$, and $\Theta > 0$, the proof is complete. \blacksquare

In the proofs that follow, for a given t we define

$$S^t = \{i : \phi_i(x^t|z^t) \leq \phi_L^t\} \quad \text{and} \quad B^t = \{i : \phi_i(x^t|z^t) > \phi_L^t\}.$$

Lemma 2.6 *Suppose that at iteration t the algorithm does not stop on line 6. Then the cut on line 9 is violated by (x^t, ϕ_L^t) by more than $\frac{\sum_{i \in B^t} e^{\alpha \phi_i(x^t|z^t)}}{\sum_{i \in I} e^{\alpha \phi_i(x^t|z^t)}} \Delta/2$.*

PROOF: It suffices to show that

$$\sum_{i \in I} e^{\alpha \phi_i(x^t|z^t)} \phi_L^t + \sum_{i \in B^t} e^{\alpha \phi_i(x^t|z^t)} \Delta/2 < \sum_{i \in B^t} e^{\alpha \phi_i(x^t|z^t)} \phi_i(x^t|z^t), \quad \text{i.e., that} \quad (13)$$

$$\sum_{i \in S^t} e^{\alpha \phi_i(x^t|z^t)} \phi_L^t < \sum_{i \in B^t} e^{\alpha \phi_i(x^t|z^t)} (\phi_i(x^t|z^t) - \phi_L^t - \Delta/2). \quad (14)$$

The left-hand side is upper bounded by $|S_t| e^{\alpha \phi_L^t} \phi_L^t < |S_t| e^{\alpha(\phi_{\max}^t - \Delta)} \phi_L^t$, while the right-hand side is lower bounded by $e^{\alpha \phi_{\max}^t} (\phi_{\max}^t - \phi_L^t - \Delta/2) > e^{\alpha \phi_{\max}^t} \Delta/2$. Hence the result follows if we can argue that

$$|S_t| \phi_L^t < e^{\alpha \Delta} \Delta/2.$$

Using $|S| \leq |I|$ and Lemma 2.5, this holds because $\ln |I| + \ln \phi_U^0 \leq \alpha \Delta + \ln(\Delta/2)$, by choice of α . \blacksquare

Corollary 2.7 *Under the same assumptions as Lemma 2.6, the violation of the cut added in line 9 is at least $\Delta/4$.*

PROOF: Consider the quantity $r \doteq \frac{\sum_{i \in B^t} e^{\alpha \phi_i(x^t|z^t)}}{\sum_{i \in I} e^{\alpha \phi_i(x^t|z^t)}}$. At least one of the terms in B^t equals $e^{\alpha \phi_{\max}^t}$. If $|B^t| = 1$ then $r > \frac{e^{\alpha \phi_{\max}^t}}{e^{\alpha \phi_{\max}^t} + |S_t| e^{\alpha \phi_L^t}} > \frac{1}{1 + |I| e^{-\alpha \Delta}}$ (because $\phi_L^t < \phi_{\max}^t - \Delta$) and, by choice of α , this ratio is larger than $1/2$ which concludes the proof.

Now assume $|B^t| \geq 2$, and let p denote the *smallest* term in $\sum_{i \in B^t} e^{\alpha \phi_i(x^t|z^t)}$. In other words, we can write $\sum_{i \in B^t} e^{\alpha \phi_i(x^t|z^t)} = p + e^{\alpha \phi_{\max}^t} + q$, and so

$$r > \frac{p + e^{\alpha \phi_{\max}^t} + q}{p + e^{\alpha \phi_{\max}^t} + q + |S_t| e^{\alpha \phi_L^t}}.$$

The numerator of the derivative of this expression with respect to p equals $|S_t| e^{\alpha \phi_L^t}$ which is nonnegative, and so the expression is minimized when $p = 0$ and likewise with q . Thus, again, $r > \frac{1}{1 + |I| e^{-\alpha \Delta}}$, as desired. \blacksquare

The following result requires uniform continuity of the functions ϕ_i over Z . That is, for any $\varepsilon > 0$ there exists a $\gamma(\varepsilon) > 0$ such that, for any pair $z, w \in Z$, $\|z - w\| < \gamma(\varepsilon)$ implies $|\phi_i(x|z) - \phi_i(x|w)| < \varepsilon$ for every $x \in P$ and any $i \in I$.

Theorem 2.8 *Assume uniform continuity of the ϕ_i holds and let $\lambda \in (0, 1)$. With α chosen large enough, either Algorithm 1 terminates finitely in line 6, or we reach an iteration τ with $\phi_{\max}^\tau \leq \lambda \phi_U^0$.*

PROOF: Let $n = |I|$ and define $N > \max\{n, 2/\lambda^2\}$. Choose

$$\varepsilon = \frac{\lambda \phi_U^0 \delta}{4}, \quad \xi = \frac{\delta/2 - 2/N^2}{1 - 2/N^2} \quad \text{and} \quad \alpha \geq \frac{3 \log N}{\xi \Delta}.$$

At each iteration t , define \hat{z}^t and $\hat{\pi}^t$ as follows:

- Let $\gamma(\varepsilon) > 0$ such that the uniform continuity of functions ϕ_i over Z holds for ε . Define $Z_{\gamma(\varepsilon)} \subseteq Z$ as a $\gamma(\varepsilon)$ -net for Z , i.e. for each $z \in Z$, there exists a $z' \in Z_{\gamma(\varepsilon)}$ such that $\|z - z'\| \leq \gamma(\varepsilon)$. $Z_{\gamma(\varepsilon)}$ is guaranteed to exist since Z is compact. Finally, we define $\hat{z}^t \in Z_{\gamma(\varepsilon)}$ as the point whose $\gamma(\varepsilon)$ -ball covers z^t .
- For each j , let $\hat{\pi}_j^t$ be π_j^t rounded down to the nearest multiple of $1/N^3$.

For any t , we say that index i is *minor* if $\phi_i(x^t | z^t) \leq (1 - \xi)\phi_{\max}^t$, and *major* otherwise. By our choice of α , and since $\Delta < \phi_{\max}^t$ for every non-terminal iteration t , we have $e^{\alpha \phi_{\max}^t} > N^3 e^{(1-\xi)\alpha \phi_{\max}^t}$. Using this bound, and denoting $\pi_{\max}^t = \max_{1 \leq i \leq n} \pi_i^t$, we see that for all minor i , $\pi_i^t < \frac{1}{N^3} \pi_{\max}^t$. So

$$\sum_{i \text{ minor}} \pi_i^t < \frac{1}{N^2} \pi_{\max}^t \leq \frac{1}{N^2} \sum_{j \text{ major}} \pi_j^t.$$

Hence, since $\sum_j \pi_j^t = 1$,

$$\sum_{j \text{ major}} \pi_j^t > 1 - \frac{1}{N^2} \quad \text{and thus} \quad \sum_{j \text{ major}} \hat{\pi}_j^t > 1 - \frac{2}{N^2}, \quad \text{and therefore}$$

$$\sum_{j \text{ major}} \hat{\pi}_j^t \phi_j(x^t | \hat{z}^t) \geq \sum_{j \text{ major}} \hat{\pi}_j^t \phi_j(x^t | z^t) - \varepsilon \geq (1 - 2/N^2)(1 - \xi)\phi_{\max}^t - \varepsilon. \quad (15)$$

Since there are finitely many pairs $(\hat{z}^t, \hat{\pi}^t)$, the algorithm will eventually repeat a pair provided it has not already terminated. Let τ be such an iteration, meaning $\hat{\pi}^\tau = \hat{\pi}^t$ and $\hat{z}^\tau = \hat{z}^t$ for some $t < \tau$. Hence

$$\begin{aligned} \phi_L^\tau &\geq \sum_j \pi_j^\tau \phi_j(x^\tau | z^\tau) \geq \sum_j \hat{\pi}_j^\tau (\phi_j(x^\tau | \hat{z}^\tau) - \varepsilon) \geq \sum_j \hat{\pi}_j^\tau \phi_j(x^\tau | \hat{z}^\tau) - \varepsilon \\ &= \sum_j \hat{\pi}_j^\tau \phi_j(x^\tau | \hat{z}^\tau) - \varepsilon \geq (1 - \frac{2}{N^2})(1 - \xi)\phi_{\max}^\tau - 2\varepsilon \end{aligned}$$

where the four inequalities follow, in order, from the cut added in iteration t , the definitions of $(\hat{z}^t, \hat{\pi}^t)$, the fact that the sum of the coordinates of $\hat{\pi}$ is at most 1, and the bound in (15).

Now suppose $\phi_{\max}^\tau > \lambda \phi_U^0$, meaning we have not significantly reduced risk by iteration τ . Then, by our definition of ε , $\frac{2\varepsilon}{\phi_{\max}^\tau} \leq \frac{2\varepsilon}{\lambda \phi_U^0} \leq \frac{\delta}{2}$, and in summary,

$$\frac{\phi_{\max}^\tau - \phi_L^\tau}{\phi_{\max}^\tau} \leq \left[1 - (1 - \frac{2}{N^2})(1 - \xi) \right] + \frac{2\varepsilon}{\phi_{\max}^\tau} \leq \frac{\delta}{2} + \frac{\delta}{2} = \delta \quad (16)$$

by choice of ξ . Thus (x^τ, ϕ_L^τ) satisfies the relative convergence condition, (b), on line 6 and the algorithm will terminate. ■

2.4.1 Choosing Θ

We first discuss a generic methodology for picking the Θ parameter. We will consider specific examples below. Let $x^* = \operatorname{argmin}\{c(x) : x \in P\}$, i.e., an optimal solution to the nominal problem (1) (without loss of generality, $x^* = x^0$). Consider parameters $0 < \lambda^{lo} < \lambda^{hi} < 1$ and $0 < \xi$. Then we set

$$\Theta = \frac{c(x^*) \xi}{\Phi(x^*) (\lambda^{hi} - \lambda^{lo})}. \quad (17)$$

Lemma 2.9 *Suppose we run Algorithm 1 using (17). Assume that the algorithm does terminate in line 6 and let \hat{x} be the solution at termination.*

(i) *If $c(\hat{x}) + \Theta \Phi(\hat{x}) \leq c(x^*) + \Theta \lambda^{hi} \Phi(x^*)$, then*

$$\Phi(\hat{x}) \leq \lambda^{hi} \Phi(x^*) \quad \text{and} \quad c(\hat{x}) \leq c(x^*) \left(1 + \frac{\lambda^{hi}}{\lambda^{hi} - \lambda^{lo}} \xi \right). \quad (18)$$

(ii) *If $c(\hat{x}) + \Theta \Phi(\hat{x}) > c(x^*) + \Theta \lambda^{hi} \Phi(x^*)$, then*

$$\exists x \in P \text{ with } \Phi(x) \leq \lambda^{lo} \Phi(x^*) \text{ and } c(x) \leq (1 + \xi)c(x^*). \quad (19)$$

Proof. (i) Since $c(\hat{x}) \geq c(x^*)$ we obtain the first inequality in (18). Moreover, $\Phi(\hat{x}) \geq 0$ implies

$$c(\hat{x}) \leq c(x^*) + \lambda^{hi} \frac{c(x^*) \xi}{\lambda^{hi} - \lambda^{lo}} = c(x^*) \left(1 + \frac{\lambda^{hi}}{\lambda^{hi} - \lambda^{lo}} \xi \right). \quad (20)$$

(ii) If such an x existed, we would have $c(x) + \Theta \Phi(x) \leq (1 + \xi)c(x^*) + \Theta \lambda^{lo} \Phi(x^*) = c(x^*) + \Theta \Phi(x^*)$. ■

In other words, the algorithm either generates a solution with both greatly reduced risk exposure and slightly increased cost, or proves that there is no point with moderately tighter requirements. As an additional point, exact solution of the master problem is only needed for part (ii).

Example. Let $\lambda^{lo} = 0.5$, $\lambda^{hi} = 0.6$ and $\xi = 0.01$. Under outcome (i) $\Phi(\hat{x}) \leq 0.6 \Phi(x^*)$ while also $c(\hat{x}) \leq 1.06 c(x^*)$. And under outcome (ii) there is no $x \in P$ with $\Phi(x) \leq 0.5 \Phi(x^*)$ and $c(x) \leq 1.01 c(x^*)$.

Discussion. The analysis in Lemma 2.9 assumes that the algorithm terminates in line 6. If not, by Theorem 2.8, after a finite number of iterations we compute a point $\tilde{x} \in P$ with $\Phi(\tilde{x}) \leq \lambda^{lo} \Phi(x^*)$. Should it be the case that $c(\tilde{x})$ is only slightly larger than $c(x^*)$ then (as in case (i) of the analysis directly above) we have computed a point with significantly lower risk exposure and slightly higher cost, as desired.

What if not, that is to say, what if $c(\tilde{x})$ is larger than $c(x^*)$ by a margin that is unacceptably high? In that case we appeal to Observation 2.4, i.e., there is *no* $x \in P$ with, both, $c(x) < c(\tilde{x})$ and $\Phi(x) \leq \Phi(\tilde{x})$. This is a similar situation as in case (ii) above – here we have a proof that the goal that we decrease risk exposure to as much as $\Phi(\tilde{x})$ requires a cost increase deemed excessive.

In other words, both this last case and case (ii) above indicate that we have acted in an excessively conservative fashion – we should therefore decrease Θ . Below we will see an example in this direction. Further, should it be the case that Θ is very small, then we have a proof that the underlying system in problem (1) is one where all near-optimal solutions are subject to high risk exposure.

2.4.2 Note: the cases $\mathcal{Z} = \emptyset$ and $|\mathcal{Z}| = 1$

In either of these cases the optimization step in line 5 is void. Hence in line 8 we simply define $\pi_i^t = \frac{e^{\alpha\phi_i(x^t)}}{\sum_{j \in I} e^{\alpha\phi_j(x^t)}}$ for each $i \in I$.

2.4.3 Modifications to the algorithm

Here we describe a number of adaptations to Algorithm 1 that we have found effective from an empirical standpoint. In some cases, those modifications are also backed by theoretical guarantees.

Formally, a boosting kernel will be any algorithm that generates, at an iteration t , nonnegative *boosting weights* w_i^t for each $i \in I$, and a separation kernel on the other hand generates coefficients $\pi_i^t = \pi_i^t(w^t)$ with $\sum_{i \in I} \pi_i^t = 1$. A key point is that, for any separation kernel and any $\bar{z} \in \mathcal{Z}$, the inequality $\phi_L \geq \sum_{i \in I} \pi_i^t \phi_i(x|\bar{z})$ is valid for the risk-adjusted problem (10).

Using this language, the boosting kernel in Algorithm (1) yields the boosting weights $\phi_i(x^t|z^t)$ where z^t is an approximate solution to the log-sum-exp maximization problem in line 5. The separation kernel applies the softmax function to the quantities $\phi_i(x^t|z^t)$. However, any combination of a boosting and a separation kernel yields a valid algorithm, and its effectiveness should be judged from an empirical perspective. We have experimented with several such variants, as follows.

Greedy method. Here the boosting kernel simply selects

$$(z^t, i^t) = \operatorname{argmax}_{z \in \mathcal{Z}, i \in I} \phi_i(x^t|z)$$

and assigns weights $w_{i^t}^t = 1$ and $w_i^t = 0$ for all other i , and the separation kernel sets $\pi_{i^t}^t = 1$ and $\pi_i^t = 0$ otherwise, that is to say the cut added on line 9 is:

$$\phi_L \geq \phi_{i^t}(x|z^t).$$

Note that $\pi^t = \operatorname{SOFTMAX}(1, w^t)$.

Lemma 2.10 *Let $\pi \in (0, 1)$. Consider Algorithm 1 using the greedy method, and suppose $0 < \lambda < 1$. Either this algorithm terminates finitely in line 6, or we reach an iteration t with $\phi_{\max}^t \leq \lambda \phi_U^0$.*

Flattening. The purpose of the boosting step at an iteration t is to highlight larger feature values in the resulting cut deployed in the separation step (i.e., larger $\phi_i(x^t|z^t)$ results in larger π_i^t). However, while the boosting accentuates order-of-magnitude differences in feature values, we also want the boosting to be less sensitive to small differences. Additionally, the numerical task in line 5 may become difficult when feature values are high. *Flattening*, when deployed, addresses both goals. It replaces each nominal feature value $\phi_i(x^t|z)$ by its logarithm $\ln \phi_i(x^t|z)$.

Synthetic boosting. When $\mathcal{Z} = \emptyset$, Algorithm 1 skips the boosting step altogether. An alternative is to rely on a *synthetic* set $\mathcal{Z}^{\text{synth}} \subset \mathbb{R}_+^I$, and to define (for example) $\phi_i(x|z) = z_i + \phi_i(x)$. Hence the boosting step approximately solves

$$\max_{z \in \mathcal{Z}^{\text{synth}}} \sum_{i \in I} e^{\alpha(z_i + \phi_i(x^t))}. \quad (21)$$

Appropriate examples for $\mathcal{Z}^{\text{synth}}$ include “budgets” sets $\{z \in \mathbb{R}_+^I : z_i \leq \gamma_i \forall i, \sum_i z_i \leq \Gamma\}$ and ball sets $\{z \in \mathbb{R}_+^I : \sum_i z_i^2 \leq \Gamma\}$.

Log-barrier term. When using synthetic boosting, we have found it empirically useful to add, to the objective function (21) log-barrier terms to prevent the optimal ζ_i values from reaching an extreme point of the set $\mathcal{Z}^{\text{synth}}$, i.e., to encourage the solution to the maximization problem to boost multiple features, which will as a result appear in the corresponding cut.

When, e.g., \mathcal{Z} is the budgets set described above, the log-barrier contribution added to the boosting problem takes the form $\varepsilon \ln(\Gamma - \sum_i z_i) + \sum_i \varepsilon_i \ln(1 - z_i)$ for positive constants $\varepsilon, \varepsilon_i (i \in I)$.

Clipping. Depending on the separation kernel, the cuts we obtain may be very dense when $|I|$ is large. This fact hinders the solution of the master problem. Additionally, many of the cut coefficient may be very small, further challenging solvers. *Clipping*, at an iteration t , works as follows:

1. Pick a (small) integer K .
2. Reset all but the top K values π_i^t to zero.
3. The top K π_i^t are proportionally reweighed so that they add to 1.

When $K = 1$, this amounts to using the cut $\phi_L \geq \phi_{i^t}^t(x|z^t)$, where $i^t = \operatorname{argmax} \phi_i(x^t|z^t)$, which coincides with the greedy cut.

2.5 Introductory examples

Here we present simple examples where Algorithm 1 or heuristics are applied to optimization problems. More substantial computations are presented later.

2.5.1 Flow routing with queueing delays

Consider a minimum-cost flow problem with a single source s and a single destination t . There are m arcs, and each arc i has a capacity u_i and a per-unit flow cost c_i , and there are $M > 0$ units of flow to route from s to t .

In addition, when flow x_i is routed on arc i , the *queueing delay* experienced on this arc equals

$$\phi_i(x_i) = \mu(u_i, x_i) \doteq \frac{u_i}{u_i + \varepsilon - x_i},$$

where $\varepsilon > 0$ (and small) is used to avoid division by zero².

We apply Algorithm (1) using the cost function $c(x) \doteq \sum_i c_i x_i$ and impact function $\Phi(x) = \max_i \phi_i(x_i)$. (Thus, $\mathcal{Z} = \emptyset$.)

As an example, consider the network with two nodes (i.e., s and t) and three parallel arcs between s and t with data as follows

arc, i	1	2	3	4
capacity, u_i	70	31	50	50
per-unit cost, c_i	1	5	7	8

There are $M = 100$ units of flow to route. Thus, the nominal optimization to solve is:

$$\begin{aligned} \min \quad & x_1 + 5x_2 + 7x_3 + 8x_4 \\ \text{s.t.} \quad & x_1 + x_2 + x_3 + x_4 = 100 \\ & 0 \leq x_1 \leq 70, 0 \leq x_2 \leq 31, 0 \leq x_3 \leq 50, 0 \leq x_4 \leq 50, \end{aligned}$$

²The function $\mu(u, x)$ is the M/M/1 queueing delay on a channel with capacity u and data rate x . See [24]

with optimal solution $x^0 = (70, 30, 0, 0)$ attaining cost 220. We set $\varepsilon = 0.01$. Thus, the maximum queueing delay is attained on arc 1 and it equals $\mu(70, 70) = 100$.

To obtain the master problem we need to add the Φ_L variable to the nominal optimization problem; additionally, we need to represent the quantity $\phi_i(x_i)$ for each $i = 1, 2, 3$. This is done by introducing a variable q_i as a proxy for $\phi_i(x_i)$ together with the inequalities

$$q_i \geq \mu(u_i, x_i) \quad (= u_i / (u_i + \varepsilon - x_i)), \quad i = 1, 2, 3,$$

which are convex-representable.

Following section 2.4.1 to set Θ , we choose $\lambda^L = 0.5$, $\lambda^U = 0.6$ and $\xi = 0.01$. Using $c(x^0) = 220$ and $\Phi(x^0) = 100$, we obtain $\Theta = 0.22$. In summary, the master problem is initialized as:

$$\begin{aligned} \min \quad & x_1 + 5x_2 + 7x_3 + 8x_4 + 0.22\Phi_L \\ \text{s.t.} \quad & x_1 + x_2 + x_3 + x_4 = 100 \\ & q_1 \geq \mu(70, x_1), \quad q_2 \geq \mu(30, x_2), \quad q_3 \geq \mu(50, x_3), \quad q_4 \geq \mu(50, x_4) \\ & 0 \leq x_1 \leq 70, \quad 0 \leq x_2 \leq 31, \quad 0 \leq x_3 \leq 50, \quad 0 \leq x_4 \leq 50, \quad \Phi_L \geq 0. \end{aligned}$$

Finally, we heuristically set $\alpha = 1/10$. The algorithm proceeds as follows.

1) Since $\mathcal{Z} = \emptyset$, line 5 of the algorithm simply amounts to evaluating $\Phi(x^0)$. As per line 8 of the algorithm, the cut we obtain on line 9 is (values rounded to three digits)

$$\phi_L \geq 0.980q_1 + 0.018q_2,$$

where we have ignored very small (but positive) coefficients on x_3 and x_4 .

2) Resolving the master problem with the added cut yields the solution vector $x_1^1 = 69.005$, $x_2^1 = 30.995$, $x_3^1 = x_4^1 = 0$ and $\phi_L^1 = 42.266$; its cost is $c(x^1) = 223.980$. Evaluating queueing delays, we have $\Phi(x^1) = 41.297$.

We note the small gap between ϕ_L^1 and $\Phi(x^1)$: the formal algorithm is close to termination as per line 6. However, the central point here is that

- (a) Comparing $\Phi(x^0) = 100$ and $\Phi(x^1) < 41.30$ we see greatly reduced risk.
- (b) Comparing $c(x^0) = 220$ and $c(x^1) < 223.99$, we see that cost has increased by less than 1.5%.

As per our goal of "substantially reducing risk without materially increasing cost" we can terminate the algorithm. Note that both (18) and (20) are satisfied.

2.5.2 Min-cost flow under capacity reduction

Consider the generic single-source, single-destination min-cost flow setup with M units of flow to route. Here we consider the case where there is a set \mathcal{Z} of *decreased capacity vectors*. Each $z \in \mathcal{Z}$ has an entry z_{uv} corresponding to each arc (u, v) , with value indicating the capacity of (u, v) in an adverse scenario that is realized after the choice of flow vector x has been made, and which impacts multiple arcs at once.

Specifically, given a flow vector x , we assume that the capacity in each arc (u, v) is (adversarially) reduced to $\min\{x_{uv}, z_{uv}\}$. As a result, some of the M units flow originally routed from s to

t using flow vector x may be lost, even if we reroute using the reduced capacities. This model incorporates a form of recourse which we have selected for this example to highlight the behavior of our algorithm. An alternative would have been to use capacities z_{uv} rather than $\min\{x_{uv}, z_{uv}\}$ – the version we selected is more constrained in terms of recourse.

Formally, given a flow vector x we proceed as follows. For each vector $z \in \mathcal{Z}$,

- (a) Let $F(x|z)$ denote the maximum flow that can be routed from s to t in the network where each arc (u, v) has *effective capacity* $\min\{x_{uv}, z_{uv}\}$. Then $F(x|z) \leq M$.
- (b) For each subset of the nodes S with $s \in S$ and $t \notin S$ let $\delta^+(S)$ be the set of arcs (u, v) with $u \in S$ and $v \notin S$. We write $\text{cap}_S(x|z) = \sum_{(u,v) \in \delta^+(S)} \min\{x_{uv}, z_{uv}\}$ to denote the *effective capacity* of the cut, i.e., the cut-capacity using the arc capacities in (a). For such a cut define $\phi_S(x|z) = \max\{M - \text{cap}_S(x|z), 0\}$. In our terminology, there is a feature for each cut.
- (c) Let \mathcal{C} be the set of cuts as in (b). We set $\phi(x|z) = \max_{S \in \mathcal{C}} \phi_S(x|z)$. We have $\phi(x|z) > 0$ if the effective capacities $\min\{x_{uv}, z_{uv}\}$ do not allow M units of flow to be routed from s to t .

In summary, we write $\Phi(x) = \max_{z \in \mathcal{Z}} \phi(x|z)$ where we assume that \mathcal{Z} is compact³. If \mathcal{Z} is finite the risk-adjusted problem (7) has an explicit linear representation. However, if \mathcal{Z} is large this representation will be prohibitively large both in terms of constraints and variables.

Next we describe our implementation of these ideas in a numerical example, given by the network in Figure 3, where we have to route $M = 100$ units of cost from s to t .

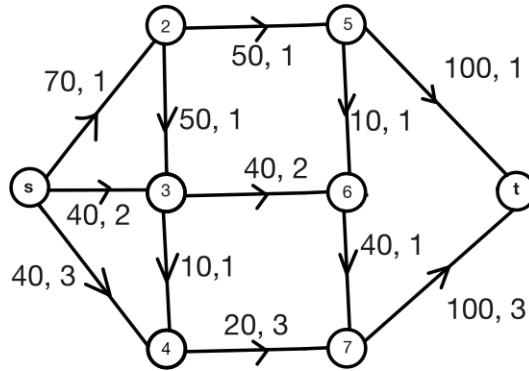


Figure 3: Reduced capacity example. For each arc we list capacity and per unit cost.

For the sake of simplicity, the reduced capacity model we use is that in each $z \in \mathcal{Z}$ up to two arcs of the network have their capacity reduced by (exactly) 50% with no other reductions. For a flow vector x the computation of $\Phi(x)$ can be modeled by a linear mixed-integer program, using binary variables to indicate the arcs where capacity is reduced, and using the dual representation of the min-cut problem – the *dual MIP* in what follows.

We use the greedy method (Section 2.4.3) and we add only one inequality to the master at each iteration. After initializing the master problem as the min cost flow problem on the given network the algorithm proceeds as follows:

³If \mathcal{Z} is finite and each $z \in \mathcal{Z}$ has a probability p_z then we could instead consider $\Phi(x) = \sum_{z \in \mathcal{Z}} p_z \phi(x|z)$. An example is that where we allow a full min-cost flow recomputation once the decreased capacities are realized.

Iteration 0. Nominal solution x^0 .

arc	(s,2)	(s,3)	(s,4)	(2,3)	(3,4)	(2,5)	(3,6)	(4,7)	(5,6)	(6,7)	(5,t)	(7,t)
flow	60	40	0	10	10	50	40	10	0	40	58	50

The optimal cost is $c(x^0) = 560$. The dual MIP sets $z_{s,2}^0 = 35$ and $z_{s,3}^0 = 20$ as the two reduced capacities. The cut separating s from the rest of the network is a min effective capacity cut, with effective capacity $z_{s,2}^0 + z_{s,3}^0 + x_{s,4} = 55 + x_{s,4} = 55$. Hence $\Phi(x^0) = 100 - 55 = 45$. Hence we add, to the master problem, the cut $\phi_L + 55 + x_{s,4} \geq 100$.

Also, using $\lambda^{lo} = 0.7$, $\lambda^{hi} = 0.75$ and $\xi = 0.01$ (17) sets $\Theta = 2.49$.

Iteration 1 yielding x^1 .

arc	(s,2)	(s,3)	(s,4)	(2,3)	(3,4)	(2,5)	(3,6)	(4,7)	(5,6)	(6,7)	(5,t)	(7,t)
flow	70	10	20	20	0	50	30	20	0	30	50	50

This solution has cost 570 and it estimates $\Phi_L = 25$. The dual MIP sets $z_{s,2}^1 = 35$ and $z_{2,5}^1 = 25$, and the minimum effective-capacity cut separates node s from the rest of the network. Its effective capacity equals $z_{s,2}^1 + x_{s,3}^1 + x_{s,4}^1 = 35 + 30 = 65$ and therefore $\Phi(x^1) = 35$. We add to the master the inequality $\phi_L + x_{s,3} + x_{s,4} \geq 65$.

Iteration 2 yielding x^2 .

arc	(s,2)	(s,3)	(s,4)	(2,3)	(3,4)	(2,5)	(3,6)	(4,7)	(5,6)	(6,7)	(5,t)	(7,t)
flow	60	20	20	10	0	50	30	20	0	30	50	50

The solution to the master problem has cost 570 and $\phi_L = 25$. The min-effective capacity cut now separates nodes $s, 2, 3$, and 4 from the rest, with $z_{2,5}^2 = 25$ and $z_{3,6}^2 = 20$, and effective capacity $45 + x_{4,7}^2 = 20 = 65$. Hence $\Phi(x^2) = 35$. Note that the reduced capacity of the adversarial cut is $25 + 20 + x_{4,7} = 45 + x_{4,7}$; however, $x_{3,6}^2 = 30$, so x^2 only loses 10 units of flow when the capacity of $(3,6)$ is reduced to 20 units (as in the current dual MIP solution). The inequality we add to the master is $\phi_L + x_{4,7} \geq 45$.

Iteration 3 yielding x^3 .

arc	(s,2)	(s,3)	(s,4)	(2,3)	(3,4)	(2,5)	(3,6)	(4,7)	(5,6)	(6,7)	(5,t)	(7,t)
flow	70	20	10	20	10	50	30	20	0	30	50	50

The solution to the master has cost $c(x^3) = 570$ and $\Phi_L = 35$. The dual MIP now sets $z_{s,2}^3 = 35$ and $z_{2,5}^3 = 25$, but only achieves $\Phi(x^3) = 35$ units of lost flow (again using the cut that separates s from the rest of the network). Since $\Phi(x^3) = \Phi_L$ the algorithm terminates.

In summary,

$$\Phi(x^3)/\Phi(x^0) = 35/45 \approx 0.78 \text{ and } c(x^3)/c(x^0) = 570/560 \approx 1.0179.$$

At the same time, we note that $c(x^3) + \Theta\Phi(x^3) = 570 + 2.49 * 35 = 657.15 > 644.0375 = c(x^0) + \Theta\lambda^{hi}\Phi(x^0)$. Consequently, by Lemma 2.9 (ii), we conclude that

$$\nexists \text{ feasible flow } x \text{ with } \Phi(x) \leq 0.7\Phi(x^0) \text{ and } c(x) \leq 1.01c(x^0).$$

3 Numerical experiments

Here we describe testing of our algorithms on large problem instances arising in two settings: operation of power grids, and logistics.

3.1 Logistics under concentration risk

In this section we apply our methodology to an evolved version of the logistical setup described in [23], which arose from an engagement with a stakeholder, and where a heuristic version of Algorithm 1 was applied. In brief, the problem being considered has the following attributes.

- Multiple commodities are shipped from sources to destinations in a network, using multiple vehicle types. The different commodities have numerical priorities and delivery time windows with lateness penalties. Vehicles have restricted availability (when and where).
- In the numerical instance considered here, there are 44 time periods; the network has 17 nodes and 224 links; there are 94 commodity types and 6 vehicle types.
- The resulting MIP formulation has 417,330 variables of which 5,920 are integral and there are 118,343 constraints. Gurobi v12 [20] was used to obtain a solution within 5% of optimality while requiring a few minutes of computation.
- It was observed, across multiple instances of the problem, that the computed MIP solution exhibits a high degree of concentration; see Figures 1 and 2. This feature was deemed (by the stakeholder) to be risk-inducing.

We have applied the methodology in this paper as follows. First, for a solution vector x in the MIP, and for an arc (i, j) and time period τ , we write $\phi_{i,j,\tau} = \phi_{i,j,\tau}(x)$ total weight of all commodities shipped on (i, j) starting at time τ under solution x . Here, a commodity's "weight" is defined as the product of the numerical priority times the actual shipped weight. We have also considered, using the same methodology, the case where $\phi_{i,j,\tau}$ only accounts for shipped weight.

For these experiments we used the following version of Algorithm 1:

1. The risk term we focused on was $\Phi(x) = \max_{i,j,\tau} \phi_{i,j,\tau}(x)$, i.e., max shipped weight, on any link and any point in time.
2. We used flattening, synthetic boosting, and log-barrier terms – see Section 2.4.3 and equation (21). Flattening is needed because the $\phi_{i,j,\tau}$ values can be large, as can be the number of triples (i, j, τ) , and we used a synthetic set because there is no overt uncertainty in the model. We relied on $\mathcal{Z}^{\text{synth}} = \{\zeta_{i,j,\tau} \geq 0 : \sum_{i,j,\tau} \zeta_{i,j,\tau} \leq 1\}$. Furthermore, we used $\alpha = 1$. Thus, at iteration t of Algorithm 1, the boosting step (approximately) solves:

$$\max_{\zeta \in \mathcal{Z}^{\text{synth}}} \left[\sum_{i,j,\tau} e^{\zeta_{i,j,\tau}} \phi_{i,j,\tau}(x^t) + \varepsilon \ln \left(1 - \sum_{i,j,\tau} \zeta_{i,j,\tau} \right) + \sum_{i,j,\tau} \varepsilon_{i,j,\tau} \ln(1 - \zeta_{i,j,\tau}) \right], \quad (24)$$

where $\varepsilon > 0$ and $\varepsilon_{i,j,\tau} > 0$ for every triple (i, j, τ) .

3. This optimization task was addressed using a first-order algorithm detailed below in Section 3.1.1. The algorithm was implemented in multistart fashion, using parallel processing.
4. Each start yields a different vector $\zeta \in \mathcal{Z}^{\text{synth}}$. The resulting SOFTMAX cut was added to the master problem if violated.

5. We used $\Theta = c(x^*)/\Phi(x^*)$. This is consistent with (17) when $\xi = \lambda^{\text{hi}} - \lambda^{\text{lo}}$.
6. Algorithm 1 was run using the LP-relaxation of the MIP. Upon termination, the MIP, with cuts added, was then run.

Iteration	Risk	Cost	Cuts	Time (s)
0	66724	1095	132	25.62
1	53992	1179	196	28.84
2	39969	1153	216	30.59
3	50437	1153	229	30.61
4	50385	1153	234	30.77
5	44181	1156	234	29.13
MIP	44181	1186		91.65

We highlight that the MIP attains a 33.33% decrease in risk metric while incurring an 8.3% increase in cost. In fact, in hindsight, we could have terminated the algorithm in iteration 2 where the performance is clearly better both in terms of risk and cost.

Table 1: Comparison: cumulative weight shipped in top activities, in units of 10^5

# of activities, K	1	2	4	8	10	16	32	64	100
nominal	3.45	6.79	12.19	20.51	23.99	33.24	45.08	52.72	53.72
risk-aware	1.45	2.91	5.82	11.63	14.54	23.26	38.37	50.80	54.23

Table 1 complements Figure 2. It displays the weight shipped in the top K activities for both the nominal and risk-aware solutions, for selected values of K up to 100, which accounts for nearly all the shipments. We remind the reader that some 150 activities have positive weight in both solutions (out of, potentially, over 10,000). We highlight the high concentration evident in the nominal solution: for example, the top ten activities account for nearly 50% of all shipped weight. In contrast, the risk-aware solution reduces the concentration metric by roughly 50 for $K < 10$, and gradually catches up with the nominal solution – while incurring a relatively small increase in cost.

3.1.1 First-order method for boosting problem

The boosting problem (24) is solved via a custom multi-start first-order ascent algorithm (henceforth termed the *Red* solver) based on AdaDelta [30], so as to handle the optimization problem (24). A first-order approach is used to permit scaling to very large instances due to empirical evidence for superior performance over nonlinear solvers (Knitro, for instance, has difficulty converging due to the interaction between the exponential and log-barrier terms). We relied on AdaDelta [30] to self-calibrate the sensitive choice of step size and to prevent stalling, and multistarting was employed to generate multiple runs per boosting step. We provide further details next.

- The feature values, $\phi_{i,j,\tau}(x^t)$, of the current solution are scaled upwards (**how**) to prevent the log-barrier terms from dominating the objective.
- Let n_{runs} be the number of runs. For each run $1 \leq h \leq n_{\text{runs}}$ we select a starting point ζ^h using a sliding window, W^h , of size $\text{window}_{\text{size}}$ and step $\text{window}_{\text{step}}$, on the sorted indices of feature values. The values $\zeta_{i,j,\tau}^h$ for (i, j, τ) within the window W^h are set to a small constant z^h whereas those outside are set to zero. Optionally, values $\zeta_{i,j,\tau}^h$ among the $\text{warmstart}_{\text{size}}$ largest feature values $\phi_{i,j,\tau}(x^t)$ with (i, j, τ) within the window are set to a larger constant $w_{\text{warmstart}}$.

- Moreover, the gradients of coordinates $\zeta_{i,j,\tau}$ outside of the window are filtered out of the first-order update computation, thus fixing these coordinates for the entirety of the run.

Worker processes are used to parallelize the solve of each initial point via a custom implementation of AdaDelta using projection and backtracking for feasibility. Projection is used to prevent variables from becoming negative, and is implemented via clipping. Conversely, backtracking is employed if a variable would cause the argument for a log function to become negative, and is implemented so as to satisfy Wolfe conditions [26].

The disparity in which corrective measure to use for the opposite sides of the feasible boundary is based on our belief that the ζ variables approaching their upper bounds indicate features worth disrupting and so merit a delicate analysis, whereas those approaching 0 are unappealing to Red and can be discarded.

In our runs we used $\varepsilon = \hat{\varepsilon} = 1$, number of runs $n_{\text{runs}} = 30$, sliding window $\text{warmstart}_{\text{size}} = 10$ and $\text{window}_{\text{step}} = 1$, support initialization constant $w_{\text{support}} = \text{number of features}/10$, warmstart constant $w_{\text{warmstart}} = 0.5$, and AdaDelta decay rate of 0.09.

3.2 ACOFP under large branch loading and thermal risk

The ACOFP (Alternating Current Optimal Power Flow) problem arises in the operation of power grids, and has received considerable attention in part due to the increasing importance of efficient energy delivery, and also because of a perceived increase in failures of grids. To put the risk issue into perspective, a standard operating requirement for power grids is that they be able to tolerate the failure of any one component (for any reason whatsoever) and this requirement is incorporated into optimization algorithms in daily use. A more evolved risk attitude focuses on a variety of flavors, including thermal management issues, and we address that perspective in this section.

For background on ACOFP and related issues, see [15], [14], [7], [8], [25], [16]. For the purpose of explaining the experiments described here, we provide a brief outline of the problem and its risk implications, using a mix of power systems and generic terminology.

- The problem seeks to generate power at minimum cost, subject to satisfying a set of demands, and physical constraints.
- As input to the problem there is a network (in the graph theoretic sense) whose *branches* (i.e., arcs) model transmission lines and are endowed with numerical parameters that describe the power flow physics.
- Power is generated at the nodes of the network, where generators are housed; each generator is described by a (convex) cost function and a maximum output. Demands are also situated at the nodes of the network.
- Power flows on branches are described by nonlinear and nonconvex equations involving physical quantities (voltages) which are also variables and are nodal attributes.
- For each branch (k, m) the power flowing from k to m is indicated by a variable P_{km} ⁴.
- Each branch (k, m) has a *resistance* $r_{km} > 0$, and the thermal energy radiated by the line is, approximately, $r_{km} P_{km}^2$ under standard assumptions on voltages (a more accurate representation is provided by the *current* on branch (k, m)).

⁴A technical detail is that, in general, $P_{km} \neq -P_{mk}$ though the difference is small.

- There is a standard approximation (not a relaxation) to ACOPF that is linear: the so-called DC approximation, or DCOPF in short, which is in fact the standard formulation used in economic grid operation (even if ACOPF is more accurate and used primarily for generic risk assessments). DCOPF does include quantities playing the role of the P_{km} above, and has identical cost function as ACOPF.

In the experiments that we describe in this section, cost (i.e., the $c(x)$ in our formulations) will be the generation cost. We will use x to generically refer to the set of all variables in ACOPF. To describe the impact function $\Phi(x)$ we rely on setups using the $r_{km} P_{km}^2$ thermal quantities described above. In what follows we write

$$T_{km} = T_{km}(x) \doteq r_{km} P_{km}^2$$

for brevity. Also let \mathcal{B} denote the set of branches of the network. Here we describe three different types of experiments, using a combination of $\Phi(x)$ functions, without and with a set \mathcal{Z} , and using different boosting and separation approaches. Some common details are as follows:

1. In all cases we compute the quantity Θ as per (17): $\Theta = \frac{c(x^*)\xi}{\Phi(x^*)(\lambda^{\text{hi}} - \lambda^{\text{lo}})}$, with $\xi = 0.01$, $\lambda^{\text{lo}} = 0.4$ and $\lambda^{\text{hi}} = 0.5$.
2. To set α in Algorithm 1 we used the following heuristic (which is aligned with the theory presented above). Let $T^* = \max_{km} T_{km}$ in the nominal case. Then $\alpha = \min\{50, \ln|\mathcal{B}|/(0.25\Phi(x^*))\}$. The demoniator in this last expression was motivated by empirical observations using relevant examples.
3. The algorithm is run until it terminates, or it achieves $\Phi_L \leq 0.5 \Phi_U^0$.
4. The algorithm is run using the DCOPF formulation which is addressed using Gurobi. Upon termination, the cuts are transferred to the ACOPF formulation and we run Knitro [13] using the amplpy [1] interface to handle that problem. We also run Knitro on the nominal ACOPF formulation in order to obtain the nominal cost and risk values.
5. With regards to the item above, an important perspective here is that while the AC formulation is clearly better aligned with power flow physics, the energy markets actually rely on the DC formulation. In light of that fact the DC-based approach is in a precise sense more meaningful, but we include the AC-based analysis for completeness.

In the experiments described below, we used the following well-known cases present in the Matpower [31] or pglib [2] libraries:

#	name	nodes	branches	generators
1	pglib_opf_case13659_pegase_api.m	13659	20467	4092
2	pglib_opf_case30000_goc_api.m	30000	35393	3526

These cases have the following attributes:

#	variables, AC	constraints, AC	variables, DC	constraints, DC
1	137837	170587	51878	47785
2	222878	307751	98920	95393

3.2.1 Introductory case with $\mathcal{Z} = \emptyset$ and maximum thermal metric

First we use

$$\Phi(x) = \max_{(k,m) \in \mathcal{B}} T_{km}.$$

Thus, there is a feature per branch, and since $\mathcal{Z} = \emptyset$ the boosting step (line 5 of Algorithm 1) is void. In terms of the cut used in the algorithms, we define

$$\pi_{km} = \frac{e^{\alpha T_{km}}}{\sum_{(k',m') \in \mathcal{B}} e^{\alpha T_{k'm'}}},$$

that is to say, $\pi = \text{SOFTMAX}(1, T)$. The coefficients π_{km} are rounded to zero if they fall beneath 10^{-6} . We obtained the following results.

#	iterations	runtime (s)	risk reduction, %	cost increase, %	AC risk reduction, %	AC cost increase, %
1	4	5.63	50.18	0.56	31.91	0.44
2	3	6.6	47.86	0.80	28.64	0.48

Note the relative degradation of the improvement in the risk metric when we go from the DC to the AC formulation.

3.2.2 Max thermal metric under distributionally robust exogenous risk

Next we consider a variant of the above max thermal feature with a significant difference. Namely, we assume that the thermal metric $T_{km} = r_{km} P_{km}^2$ is now augmented with a term that reflects an exogenous source of risk. Briefly, elevated transmission line temperatures pose a number of risks that are difficult to quantify. Additionally, line temperatures are due to a combination of endogenous factors (our T_{km} term, in approximation) and exogenous and uncertain factors that are extremely difficult to precisely specify and measure. See the IEEE 738 standard [21].

Both factors, endogenous and exogenous, are nominally combined using the heat equation, whose (deterministic) solution would yield line temperature as a function of time – once more, an effectively impossible task due to data unavailability to the operator. As a final point, it is worth stressing that under such a model, actual line temperature on an branch (k, m) is a highly nonlinear function of T_{km} and the exogenous factors.

We take a stance where we measure actual risk by adding, to the T_{km} term, a second term that reflects a given multiple of a standard deviation of additional thermal risk exposure. We assume that to first order, that additional term is *proportional* to T_{km} .

More precisely, for a branch (k, m) , we write $\phi_{km}(x|z) = (1 + z_{km})T_{km}$, where $z_{k,m} \geq 0$ is the multiplicative exogenous impact on risk. In this section we focus on the case where

$$\Phi(x) = \max_{z \in \mathcal{Z}} \max_{(k,m) \in \mathcal{B}} \phi_{km}(x|z),$$

and we will use a budgets set

$$\mathcal{Z} = \left\{ 0 \leq z_{k,m} \leq 1 : \sum_{(k,m) \in \mathcal{B}} z_{k,m} \leq N \right\},$$

for some $N > 0$. In terms of the usage of Algorithm 1, we applied the following rules:

- The solution to the boosting problem in line 5 is obtained by setting $z_{km} = 1$ for the N branches (k, m) with top value $T_{k,m}$, and $z_{k,m} = 0$ otherwise.

- We used $N = 5$, and we applied *clipping* (Section 2.4.3) when computing the cut used in the separation step. This last feature is motivated by the fact that at any given iteration t , the branches with $z_{k,m}^t = 1$ are also those with largest value $T_{k,m}$, and, as a result, the sum of the top $2N$ values $e^{\alpha(1+z_{km})T_{km}}$ strongly dominates the sum of all such terms. In other words, the top $2N$ values π_{km}^t already add up to approximately 1 (and the rest contribute a negligible amount).

#	iterations	runtime (s)	risk reduction, %	cost increase, %	AC risk reduction, %	AC cost increase, %
1	10	18.78	50.76	1.05	36.41	0.56
2	5	64.66	50.33	0.56	28.43	0.48

3.2.3 Average of top five

Let $T_{(i)} = T_{(i)}(x)$ be the i^{th} largest value T_{km} . We remind the reader that the $T_{km} = r_{km}P_{km}^2$ and that x is the vector of all variables, including the P_{km} . In the next set of experiments we use

$$\Phi(x) = \frac{1}{5} \sum_{i=1}^5 T_{(i)}.$$

This is again a case with $\mathcal{Z} = \emptyset$. If we use \mathcal{B}^5 to denote the set of all 5-tuples chosen from \mathcal{B} , we can equivalently write

$$\Phi(x) = \max_{s \in \mathcal{B}^5} \phi_s(x), \quad \text{where for } s \in \mathcal{B}^5 \text{ we write } \phi_s(x) = \frac{1}{5} \sum_{(k,m) \in s} T_{km}. \quad (25)$$

In other words, there is a feature for each 5-tuple of branches. For the separation step we used the following approach:

- At any iteration t we generate a set $S^t \subset \mathcal{B}^5$.
- We construct S^t by selecting 5-tuples chosen from among the top 15 branches (k,m) as per the metric T_{km} . The set S^t is guaranteed to include the tuple s attaining maximum value $\phi_s(x^t)$ as in (25).
- For each tuple $s \in S^t$ we add the cut $\phi_L \geq \frac{1}{5} \sum_{(k,m) \in s} T_{km}$. Thus, with $|S^t| = 10$, ten cuts are added in each iteration.

#	iterations	runtime (s)	risk reduction, %	cost increase, %	AC risk reduction, %	AC cost increase, %
1	4	11.22	50.54	1.16	38.69	0.87
2	10	39.93	43.22	0.88	29.11	0.91

3.2.4 Average of top five under distributionally robust exogenous risk

Here we continue with the model above, but, as in Section 3.2.2, we use a multiplicative model for endogenous risk.

More precisely, for a tuple $s \in \mathcal{B}^5$ we write

$$\phi_s(x|z) = \frac{1}{5} \left(\sum_{(k,m) \in s} (1 + z_{km}) T_{km} \right),$$

where $z_{km} \geq 0$ is the multiplicative exogenous impact on (k, m) . Continuing as above, we will now focus on

$$\phi(x|z) = \max_{z \in \mathcal{Z}} \max_{s \in \mathcal{B}^5} \phi_s(x|z) = \max_{z \in \mathcal{Z}} \max_{s \in \mathcal{B}^5} \frac{1}{5} \left(\sum_{(k,m) \in s} (1 + z_{km}) T_{k,m} \right).$$

For these experiments we used

$$\mathcal{Z} = \{z \in \mathcal{B} : \|z\|_2 \leq 1\},$$

i.e., the Euclidean unit ball. In terms of implementation of Algorithm 1 we used the following methodology:

- The boosting step used the greedy method, that is to say, at iteration t we set

$$z^t = \operatorname{argmax}_{\|z\|_2=1} \max_{s \in \mathcal{B}^5} \sum_{(k,m) \in s} z_{km} T_{km} = \operatorname{argmax}_{\|z\|_2=1} \sum_{(k,m) \in s^*} z_{km} T_{km},$$

where $s^* \in \mathcal{B}^5$ is the ordered 5-tuple made up of the top 5 branches under the T_{km} metric. A computation shows that

$$z_{k,m}^t = \frac{T_{km}}{\sqrt{\sum_{(k',m') \in s^*} (T_{k',m'}^t)^2}} \text{ for } (k, m) \in s^*, \quad z_{k,m}^t = 0 \text{ otherwise.}$$

- For the cutting step we used the same approach as in the above section, i.e., we select a set of tuples s (including s^*) (a total of ten tuples in the set) and for each tuple we add the cut $\phi_L \geq \frac{1}{5} \sum_{(k,m) \in s} (1 + z_{km}^t) T_{km}$.

#	iterations	runtime (s)	risk reduction, %	cost increase, %	AC risk reduction, %	AC cost increase, %
1	10	11.92	56.78	1.34	36.26	1.03
2	12	62.66	43.39	0.88	27.20	0.81

3.2.5 Analysis of outcomes

Here we compare the solutions computed using the above models, as specific to case #2 (the 30,000-node system).

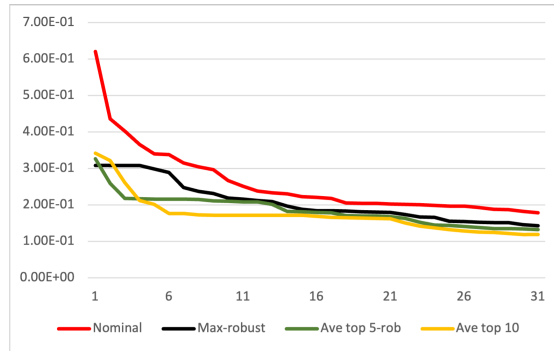


Figure 4: Thermal metrics comparison

In Figure 4 we display the top 30 values T_{km} for the solution computed in the nominal case, the max-robust case in Section 3.2.2, and the average-top-5-robust case considered in Section 3.2.4. In

addition, we are also plotting the same statistic for a run similar to that in Section 3.2.3, but using the average of the top 10 features (rather than 5). It is important to note that the 30 values plotted on each of these four curves refer, in each case, to a set of 30 *different* branches (k, m) . Nevertheless, the plots can be viewed as aggregate risk profiles.

As expected, all solutions produced by the algorithm substantially reduce the risk present in the nominal solution. The max-robust solution is the least attractive among those but even so, it continues to de-risk the nominal solution even after we move past the maximum.

Another feature of interest is that these three solutions exhibit similar maxima, but the the "max-robust solution" appears inferior to the "average of top 5 (robust)" and the "average of top 10" solutions. The latter, superficially, appears to be the most appealing, but it should be remembered that all three of the "robust" solutions have that additional attribute, i.e., they are protected against (a model of) exogenous risk.

References

- [1] AMPL Optimization Inc.: AMPL Python API (2026), <https://ampl.com>, accessed: May 23, 2026
- [2] Babaeinejadsarookolae, S., Birchfield, A., Coffrin, C., et al.: The Power Grid Library for Benchmarking AC Optimal Power Flow Algorithms. arXiv preprint arXiv:1908.02788 (2019)
- [3] Beck, Y., Ljubić, I., Schmidt, M.: Linear and Mixed-Integer Bilevel Optimization: Theory and Algorithms. Cambridge University Press (2026), <https://yasminebeck.github.io/files/bilevel-optimization-cup.pdf>
- [4] Benders, J.F.: Partitioning procedures for solving mixed-variables programming problems. *Numerische Mathematik* **4**(1), 238–252 (1962). <https://doi.org/10.1007/BF01386316>, <https://doi.org/10.1007/BF01386316>
- [5] Bertsimas, D., Brown, D.B., Caramanis, C.: Theory and applications of robust optimization. *SIAM Review* **53**(3), 464–501 (2011)
- [6] Bertsimas, D., Sim, M.: The price of robustness. *Operations Research* **52**(1), 35–53 (2004)
- [7] Bienstock, D.: Electrical transmission system cascades and vulnerability, an Operations Research viewpoint. Society for Industrial and Applied Mathematics (2015)
- [8] Bienstock, D., Escobar, M., Gentile, C., Liberti, L.: Mathematical programming formulations for the alternating current optimal power flow problem. *4OR* **18**(3), 249–292 (Sep 2020). <https://doi.org/10.1007/s10288-020-00455-w>, <https://link.springer.com/10.1007/s10288-020-00455-w>
- [9] Bienstock, D.: Potential Function Methods for Approximately Solving Linear Programming Problems: Theory and Practice, vol. 53. Springer Science & Business Media (2006)
- [10] Bienstock, D., Iyengar, G.: Solving fractional packing problems in $\mathcal{O}^*(1/\varepsilon)$ iterations. In: Proceedings of the Thirty-Sixth Annual ACM Symposium on Theory of Computing. pp. 146–155. STOC '04, Association for Computing Machinery, New York, NY, USA (2004). <https://doi.org/10.1145/1007352.1007376>

- [11] Bienstock, D., Verma, A.: The N-K problem in power grids: New models, formulations, and numerical experiments. *SIAM Journal on Optimization* **20**(5), 2352–2380 (2010)
- [12] Brown, G., Carlyle, M., Salmerón, J., Wood, K.: Defending critical infrastructure. *Interfaces* **36**(6), 530–544 (2006)
- [13] Byrd, R., Nocedal, J., Waltz, R.: Knitro: An Integrated Package for Nonlinear Optimization. In: *Large-Scale Nonlinear Optimization*, vol. 83, pp. 35–59. Springer (2006)
- [14] Cain, M.B., O’Neill, R.P., Castillo, A.: *History of Optimal Power Flow and Formulations*. Federal Energy Regulatory Commission (2012)
- [15] Carpentier, J.L.: Contribution a l’etude du dispatching economique. *Bulletin de la Societe Francoise des Electriciens* **8**, 431–447 (1962)
- [16] Coffrin, C., Van Hentenryck, P.: A linear-programming approximation of ac power flows. *INFORMS Journal on Computing* **26**, 718–734 (2014)
- [17] Cormican, K.J., Morton, D.P., Wood, R.K.: Stochastic network interdiction. *Operations Research* **46**(2), 184–197 (1998)
- [18] Fratta, L., Gerla, M., Kleinrock, L.: The flow deviation method: An approach to store-and-forward communication network design. *Networks* **3**(2), 97–133 (1973)
- [19] Grigoriadis, M.D., Khachiyan, L.G.: Fast approximation schemes for convex programs with many blocks and coupling constraints. *SIAM Journal on Optimization* **4**(1), 86–107 (1994)
- [20] Gurobi Optimization, LLC: Gurobi Optimizer Reference Manual (2026), <https://www.gurobi.com>
- [21] IEEE Power and Energy Society: IEEE Standard for Calculating the Current-Temperature Relationship of Bare Overhead Conductors. IEEE Standard IEEE Std 738-2012, IEEE, New York, NY, USA (December 2012). <https://doi.org/10.1109/IEEESTD.2012.6401981>
- [22] Kelley, J.E.J.: The Cutting-Plane Method for Solving Convex Programs. *Journal of the Society for Industrial and Applied Mathematics* pp. 703–712 (1960)
- [23] Kilb, J., Newman, A., Bienstock, D.: Probabilistic Modeling versus Robust Optimization: A tutorial based on a humanitarian logistics use case. *arXiv:2604.02493* pp. 1–46 (2026)
- [24] Kleinrock, L.: *Queueing Systems, Volume 1*. John Wiley & Sons, Inc. (1975)
- [25] Molzahn, D.K., Hiskens, I.A.: *A Survey of Relaxations and Approximations of the Power Flow Equations*. Now, Foundations and Trends (2019)
- [26] Nocedal, J., Wright, S.: *Numerical Optimization*. Springer Series in Operations Research and Financial Engineering, Springer, 2 edn. (2006)
- [27] Plotkin, S.A., Shmoys, D.B., Tardos, É.: Fast approximation algorithms for fractional packing and covering problems. In: *32nd Annual Symposium on Foundations of Computer Science, San Juan, Puerto Rico, 1-4 October 1991*. pp. 495–504. IEEE Computer Society (1991). <https://doi.org/10.1109/SFCS.1991.185411>

- [28] Salmerón, J., Wood, K., Baldick, R.: Worst-Case Interdiction Analysis of Large-Scale Electric Power Grids. *IEEE Trans. Power Systems* **24**, 96–104 (2009)
- [29] Shahrokhi, F., Matula, D.W.: The maximum concurrent flow problem. *J. ACM* **37**, 318–334 (1990), <https://api.semanticscholar.org/CorpusID:4469579>
- [30] Zeiler, M.D.: ADADELTA: An adaptive learning rate method. arXiv preprint arXiv:1212.5701 (2012)
- [31] Zimmerman, R., Murillo-Sanchez, C., Gan, D.: MATPOWER, A MATLAB Power System Simulation Package. *IEEE Trans. Power Sys.* **26**, 12–19 (2011)